Article

pubs.acs.org/Biomac

Fate of Linear and Branched Polyether-Lipids In Vivo in Comparison to Their Liposomal Formulations by ^{18}F-Radiolabeling and Positron Emission Tomography

Achim T. Reibel,[†,‡] Sophie S. Müller,[‡,§] Stefanie Pektor,[∥] Nicole Bausbacher,[∥] Matthias Miederer,[∥] Holger Frey,*[,§] and Frank Rösch*[,†]

[†]Institute of Nuclear Chemistry and [§]Institute of Organic Chemistry, Johannes Gutenberg University, Mainz, Germany
[∥]Clinic for Nuclear Medicine, University Medical Center, Mainz, Germany

Supporting Information

ABSTRACT: In this study, linear poly(ethylene glycol) (PEG) and novel linear-hyperbranched, amphiphilic polyglycerol (*hb*PG) polymers with cholesterol (Ch) as a lipid anchor moiety were radiolabeled with fluorine-18 via copper-catalyzed click chemistry. In vivo investigations via positron emission tomography (PET) and ex vivo biodistribution in mice were conducted. A systematic comparison to the liposomal formulations with and without the polymers with respect to their initial pharmacokinetic properties during the first hour was carried out, revealing remarkable differences. Additionally, cholesterol was directly labeled with fluorine-18 and examined likewise. Both polymers, Ch-PEG$_{27}$-CH$_2$-triazole-TEG-^{18}F and Ch-PEG$_{30}$-*hb*PG$_{24}$-CH$_2$-triazole-TEG-^{18}F (TEG: triethylene glycol), showed rapid renal excretion, whereas the ^{18}F-cholesten displayed retention in lung, liver, and spleen. Liposomes containing Ch-PEG$_{27}$-CH$_2$-triazole-TEG-^{18}F revealed a hydrodynamic radius of 46 nm, liposomal Ch-PEG$_{30}$-*hb*PG$_{24}$-CH$_2$-triazole-TEG-^{18}F showed a radius of 84 nm and conventional liposomes with ^{18}F-cholesten 204 nm, respectively. The results revealed fast uptake of the conventional liposomes by liver, spleen, and lung. Most importantly, the novel *hb*PG-polymer stabilized liposomes showed similar behavior to the PEG-shielded vesicles. Thus, an advantage of multifunctionality is achieved with retained pharmacokinetic properties. The approach expands the scope of polymer tracking in vivo and liposome tracing in mice via PET.

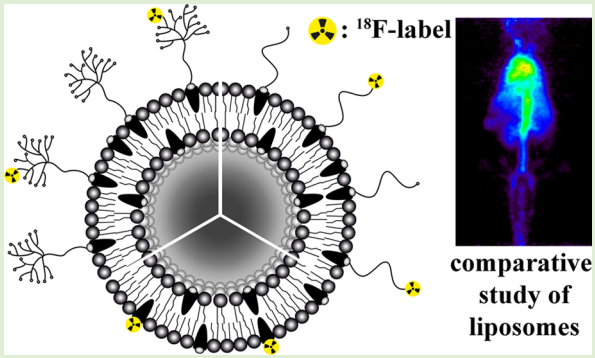

INTRODUCTION

Liposomes are spherical vesicles that consist of a phospholipid bilayer. Such systems have been intensively investigated as drug delivery vehicles with promising results.[1,2] Conventional liposomes suffer from fast removal by the mononuclear phagocyte system (MPS) via macrophages and uptake in liver and spleen, which minimizes the in vivo circulation time. Key parameters influencing the opsonization process, that is, binding of an opsonin for marking a pathogen for ingestion and phagocytosis, include liposome size, composition, and charges.[3] To overcome the drawbacks of conventional liposomes, poly(ethylene glycol) (PEG) chains are used as a stabilizing polymer shell ("stealth" liposomes).[4,5] PEG is covalently linked to cholesterol or phospholipids to ensure hydrophobic anchoring in the lipid bilayer. This protective, hydrophilic polymer layer prevents opsonin adsorption via steric repulsion.[6] Prolonged blood circulation times, reduced MPS uptake, reduced aggregation in serum, and improved (storage) stability are the main advantages of the so-called "stealth" liposomes. Nevertheless, the "gold standard" PEG suffers from disadvantages such as its nonbiodegradability, possible disintegration under stress, and potentially toxic side products, as well as causing hypersensitivity in some cases.[7] However, the main drawback of this polymer is its lack of functional groups, especially when methoxyPEG is used. Promising alternatives are highly water-soluble polymers, such as poly(vinylpyrrolidone),[8] poly(acrylamide),[8] poly(2-oxazoline),[9] zwitterionic structures,[10] and hyperbranched polyglycerol (*hb*PG). It has been shown that *hb*PG reveals enhanced protein repulsion compared to PEG.[11,12] Additionally, the branched structure renders the polymer even more bulky and more hydrophilic due to the multiple hydroxyl groups.

Maruyama et al. reported on phosphatidyl polyglycerols (oligomers) with increased circulation times,[13] and recently, our group presented a synthetic approach for linear-hyperbranched polyether lipids. Using cholesterol directly as an initiator for the oxyanionic ring-opening polymerization (ROP) of various epoxides, a variety of architectures and a tunable number of hydroxyl groups are achievable.[14,15] Cholesterol-initiated linear-hyperbranched amphiphiles combine the

Received: November 28, 2014
Revised: February 2, 2015
Published: February 3, 2015

DOI: 10.1021/bm5017332
Biomacromolecules 2015, 16, 842−851

advantageous properties of PEG and the polyfunctionality of polyglycerol with cholesterol as a natural membrane component.[16,17] Very recently, we evaluated these types of liposomes with regard to their stability in human blood serum via dynamic light scattering. No aggregation was found for liposomes stabilized with linear-hyperbranched lipids.[18] The multiple hydroxyl groups play an important role, when it comes to functionalization with markers, antibodies for "active" targeting, or radiolabels, as shown in this work.

Liposomes labeled with radioisotopes (^{99m}Tc, ^{186}Re, ^{67}Ga, ^{111}In, ^{64}Cu, ^{18}F)[19−25] were previously investigated to study the biodistribution of various types of liposomes.[26] Different routes such as membrane labeling, remote loading, encapsulation, or surface chelation are possible, but rather few ways to label the stabilizing polymer are reported.[27,28] Positron emission tomography (PET) can be used for in vivo visualization with the known advantages, such as the possibility of quantification and excellent temporal resolution. Although ^{18}F is a rather short-lived radionuclide ($t_{1/2}$ = 109.7 min), it combines ideal nuclear characteristics for PET imaging with not affecting the polymer structure, neither in size nor in charge, which is often not the case for chelating agents.[29] This tool supports the study of initial biodistribution directly after application and excretion patterns and serves as a screening platform for potential drug delivery systems.

In previous studies, incorporation of ^{18}F into long-circulating liposomes was achieved by the encapsulation of 2-[^{18}F]-2-fluoro-2-deoxy-D-glucose (2-[^{18}F]FDG) during liposome formation.[30,31] Encapsulation efficiency was around 10%.[32,33] Direct ^{18}F-labeling of 3-tosyl-1,2-dipalmitoyl glycerol by Ferrara and co-workers led to [^{18}F]fluorodipalmitin ([^{18}F]FDP), which was incorporated into the phospholipid bilayer.[34] The amphiphilic compound 1-[^{18}F]fluoro-3,6-dioxatetracosane was also used for in vivo trafficking of liposomes using PET as a noninvasive real-time imaging system.[35] In a recent work, Reiner and co-workers addressed limitations in creating targeted liposomes and the challenges for imaging,[36] where [^{18}F]FDP served as the radiolabeled lipid. The reaction between tetrazine in the treated tumor tissue and *trans*-cyclooctene at the liposome surface was employed for bioorthogonal conjugation and in vivo click chemistry. ^{18}F-Radiolabeled liposomes showed a significantly increased uptake in tetrazine-rich tumors. The synthesis of a ^{18}F-labeled cholesteryl ether lipid was recently presented by Jensen et al., who also demonstrated the visualization of radiolabeled liposomes.[37] However, in these approaches, the polymer fate in vivo is not investigated, since usually the lipids or the liposome cargo is radiolabeled. Tracking the synthetic polymer that is responsible for the enhanced circulation in the bloodstream is crucial to study the behavior and biodistribution for biomedical applications. To the best of our knowledge, there are no studies up to date that rely on labeling the stabilizing polymer by fluorine-18 via click chemistry.

In the present work, we approach this key issue and focus on the investigation of multifunctional hyperbranched cholesterol-lipids (Ch-PEG$_{30}$-*hb*PG$_{24}$) in comparison with linear PEGylated (Ch-PEG$_{27}$) ones. In addition, the liposomal formulations of these two polymers were compared with non-PEGylated (i.e., conventional) liposomes (Figure 1) labeled with ^{18}F-cholesten as a generally usable probe for liposome labeling. The polyether-based lipids were functionalized with alkyne groups by the attachment of propargyl bromide to the hyperbranched polyglycerol block in a postpolymerization reaction.[15] In the case of the linear PEG analogue, propargyl bromide was used as the end-capping agent in the oxyanionic ROP of ethylene oxide (EO, Scheme 1). The copper-catalyzed azide−alkyne cycloaddition (CuAAC) was employed for the attachment of the radiolabeled synthon 1-azido-2-(2-(2-[^{18}F]fluoroethoxy)ethoxy)ethane ([^{18}F]F-TEG-N$_3$). Compared to other investigations on sterically stabilized liposomes using PET, the main advantage of the chosen strategy is the labeling of the polymer structure itself that actually shields the liposome while profiting from the outstanding properties of ^{18}F. PET and ex vivo biodistribution studies permitted the investigation of both polymers and liposome formulations in mice.

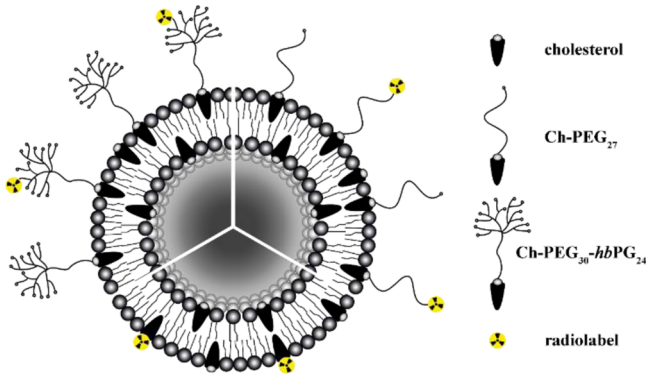

Figure 1. Conceptual design of three different types of lipids incorporated into liposomes studied in this work: cholesterol, linear poly(ethylene glycol) with a cholesterol anchor (Ch-PEG$_{27}$-CH$_2$−C≡CH), and linear-hyperbranched polyether-based lipids (Ch-PEG$_{30}$-*hb*PG$_{24}$-CH$_2$−C≡CH); all compounds were labeled with fluorine-18 for PET measurements; for a clear overview polymer chains are not drawn inside the liposome and are not drawn to scale.

EXPERIMENTAL SECTION

Instrumentation. ^{1}H NMR spectra (300 and 400 MHz) were recorded using a Bruker AC300 or a Bruker AMX400, employing MeOD or $CDCl_3$ as solvent. ^{19}F NMR analysis was carried out with a Bruker DRX-400 at 400 MHz. All spectra are referenced internally to residual proton signals of the deuterated solvent. Size exclusion chromatography (SEC) measurements were carried out in dimethylformamide (DMF) with 0.25 g L^{-1} LiBr on PSS HEMA columns (300/100/40). For SEC measurements, a UV (275 nm) and an RI detector were used. Calibration was carried out using poly(ethylene glycol) (PEG) standards provided by Polymer Standards Service (PSS). To determine the critical micelle concentration (CMC) of the polyether lipids, surface tension measurements were performed on a Dataphysics DCAT 11 EC tensiometer equipped with a TV 70 temperature control unit, a LDU 1/1 liquid dosing and refill unit, as well as a RG 11 Du Noüy ring. The Du Noüy ring was rinsed thoroughly with Millipore water and annealed in a butane flame prior to use. Surface tension data was processed with SCAT v3.3.2.93 software. The CMC presented is a mean value of two experiments. All solutions for surface tension measurements were stirred for 120 s at a stir rate of 50%. After a relaxation period of 360 s, three surface tension values were measured. During radio-synthesis a Merck LaChrom HPLC system was used with Interface D-7000, Programmable Autosampler L-7250, Pump L7100 (2×), UV-Detector L-7400, Column Oven L-3000 with manual injection rheodyne, and a Gabi Star (Raytest) for detecting activity. Radio-TLCs were analyzed by Packard Instant Imager. In ex vivo studies, fluorine-18 activities were measured using a PerkinElmer 2470 Wizard^2 γ-counter.

Solutions for light scattering experiments were prepared in a dust-free flow box. Cylindrical quartz cuvettes (20 mm diameter, Hellma, Mühlheim) were cleaned by dust-free distilled acetone. All samples

DOI: 10.1021/bm5017332
Biomacromolecules 2015, 16, 842−851

Scheme 1. Reaction Scheme for the Synthesis of Ch-PEG$_{27}$-CH$_2$-C≡CH (1) Using Cholesterol as an Initiator for the Ring-Opening Polymerization of Ethylene Oxide (EO)

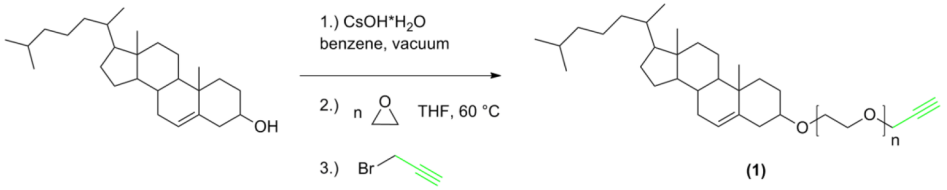

Table 1. Composition of Different Liposome Formulations[a]

	molar ratios (DOPC/cholesterol/polymer)	DOPC (mg)	polymer (mg)	cholesterol (mg)
Ch-PEG$_{27}$-^{18}F	60:20:20	13.13 (16.7 μmol)	8.8 (5.5 μmol)	2.15 (5.5 μmol)
Ch-PEG$_{30}$-*hb*PG$_{24}$-^{18}F	60:35:5	2.62 (3.3 μmol)	1.0 (0.28 μmol)	0.75 (1.9 μmol)
	60:20:20	2.62 (3.3 μmol)	4.0 (1.12 μmol)	0.43 (1.12 μmol)
^{18}F-Cholesten	60:40:0	10.51 (13.4 μmol)		3.45 (8.9 μmol)

[a]To save space, the abbreviation "CH$_2$-triazole-TEG" is left out in the description of the polymers.

(liposomes in phosphate buffered saline (PBS)) were filtered through LCR450 nm filters (Millipore) into the cuvettes. All light scattering experiments were performed with an instrument consisting of a HeNe laser (632.8 nm, 25 mW output power), an ALV-CGS 8F SLS/DLS 5022F goniometer equipped with eight simultaneously working ALV 7004 correlators, and eight QEAPD Avalanche photodiode detectors. All correlation functions were typically measured from 30 to 150° in steps of 15°, 20°, or 30° (DLS: dynamic light scattering).

Liposome Formation. Liposomes consisting of the polymer lipid (Ch-PEG$_{27}$-CH$_2$-triazole-TEG-^{18}F (**9**), Ch-PEG$_{30}$-*hb*PG$_{24}$-CH$_2$-triazole-TEG-^{18}F (**10**), or ^{18}F-Cholesten (**11**)), cholesterol and 1,2-dioleoyl-*sn*-glycero-3-phosphatidylcholine (DOPC) were prepared by the thin film hydration method on a clean bench. A solution of DOPC in ethanol, cholesterol in ethanol, and the radiolabeled copolymer/cholesten in ethanol were blended at molar ratios of 60:35:5 or 60:20:20 mol%, respectively. The objective was to keep the molar ratios of lipid and cholesterol constant. Because of the cholesteryl-anchored polymers, the total ratio of lipid to cholesterol was kept at 60:40, regardless of the amount of polymer added. The solvent was evaporated in a miniature rotating evaporator to obtain a thin film of liposome components. The lipid film was hydrated with 1 mL of PBS buffer solution to obtain the final lipid concentrations summarized in Table 1, sonicated for 10 min at 50 °C to yield large multilamellar vesicles (MLVs) and extruded through a 400 nm polycarbonate membrane 11 times. This was followed by extrusion through a 100 nm membrane for 11 times to obtain small unilamellar vesicles (SUVs) using a Mini-Extruder (Avanti Polar Lipids Inc.). Finally, the solution was purified via size exclusion chromatography (~0.5 g Sephadex G 75 packed in a 6 mL empty SPE tube with 20 μm PTFE frits at top and bottom) to separate the liposomes from not incorporated smaller molecules. Stability was proven by DLS measurements of the injected fractions.

Animal Studies. For ex vivo biodistribution and μPET studies male C57bl6J mice (Charles River Wiga, Sulzfeld, Germany; body weight 20.8–28.6 g) housed in the animal care facility of the Johannes Gutenberg-University of Mainz were used. All experiments had previously been approved by the regional animal ethics committee and were conducted in accordance with the German Law for Animal Protection and the UKCCCR Guidelines.[38]

Ex Vivo Biodistribution Studies. For ex vivo biodistribution studies, ^{18}F-labeled compounds in phosphate buffered saline solution (2.45–8.64 MBq, 100–150 μL) were injected into animals intravenously (i.v.) via tail vein. An estimation of the applied mass of polymers was done ((**9**): <1.32 mg, (**10**): <0.15 mg). After 60 min post-injection (p.i.), the animals were sacrificed and different organs (lung, blood, liver, spleen, kidneys, skeletal muscle, heart, urine, small intestine, testes) were excised. The samples were weighed and measured in a PerkinElmer 2470 Wizard^2 γ-counter to calculate the percentage of injected dose per gram tissue (%ID/g).

In Vivo Micro PET Studies. For in vivo μPET studies, the mice were anaesthetized with isoflurane (2.5%) and the fluorinated compounds were injected into a tail vein. The μPET imaging was recorded on a Focus 120 small animal PET (Siemens/Concorde, Knoxville, U.S.A.). During PET measurements, the mice were placed in a head first prone position. Dynamic PET studies were acquired in list mode. The injected activity of radiolabeled compounds was 4.74 ± 1.24 MBq (in 100–150 μL of phosphate buffered saline). An estimation of the applied mass of polymers was done ((**9**): <1.32 mg, (**10**): <0.15 mg). The PET list mode data were histogrammed into 19 frames (3 × 20 s, 3 × 60 s, 3 × 120 s, 10 × 300 s) and reconstructed using FBP algorithm with dead time correction. Scatter correction was not applied.

Reagents. All reagents and solvents were purchased from Acros or Sigma-Aldrich and used as received, unless otherwise mentioned. Anhydrous solvents were stored over molecular sieves and were purchased from Sigma-Aldrich. Deuterated solvents were purchased from Deutero GmbH, and stored over molecular sieves. Cholesterol was purchased from Acros and stored at 8 °C. Ethoxyethyl glycidyl ether (EEGE) was synthesized as described in the literature,[39] dried over CaH$_2$, and cryo-transferred prior to use. Glycidol was purified by distillation from CaH$_2$ directly prior to use. Ethanol (abs.) was purchased from Merck. Phosphate buffered saline packs were purchased from Thermo Scientific. 1,2-Dioleoyl-*sn*-glycero-3-phosphocholine (DOPC), the mini-extruder, the polycarbonate membranes, and filters were obtained from Avanti Polar Lipids. ^{18}F was delivered in ^{18}O-enriched water by the department of radiology, University Hospital Tübingen, Germany.

Polymer Syntheses. *Ch-PEG$_{27}$-CH$_2$-C≡CH (1).* Cholesterol (0.4 mg, 1.0 mmol), cesium hydroxide monohydrate (148 mg, 0.88 mmol), and benzene were placed in a Schlenk flask. The mixture was stirred at RT for about 30 min to generate the cesium alkoxide (degree of deprotonation, 85%). The salt was dried under vacuum at 90 °C for 24 h, anhydrous tetrahydrofuran (THF) was added via cryo-transfer, and ethylene oxide (2.2 mL, 44 mmol) was cryo-transferred first to a graduated ampule and then to the Schlenk flask containing the initiator solution. The mixture was allowed to warm up to room temperature, heated to 60 °C, and the polymerization was performed for 12 h at this temperature under vacuum. The reaction was cooled, quenched with propargyl bromide (0.2 mL, 1.85 mmol), and stirred for an additional 12 h. The solvent was evaporated and the crude product was precipitated into cold diethyl ether. Yield ~ 70%.

^{1}H NMR (400 MHz, CDCl$_3$) δ 5.32 (s, 1H), 4.20 (d, 2H), 3.80–3.40 (polyether backbone), 3.15 (s, 1H), 2.43 (t, 1H), 2.27–0.82 (C*H*$_2$, C*H* cholesterol), 0.66 (s, 3H).

Ch-PEG$_{30}$-hbPG$_{24}$-CH$_2$-C≡CH (2). Compound **2** was prepared and functionalized with propargyl bromide according to the literature.[14,15] Yield ~ 56%.

DOI: 10.1021/bm5017332
Biomacromolecules 2015, 16, 842–851

Scheme 2. Reaction Scheme for the Radioactive Labeling of Ch-PEG$_{27}$-CH$_2$-C≡CH (1) and Ch-PEG$_{30}$-*hb*PG$_{24}$-CH$_2$-C≡CH (2) Lipids with [^{18}F]F-TEG-N$_3$ (8) Using the Copper-Catalyzed Azide−Alkyne Reaction (CuAAC), Respectively

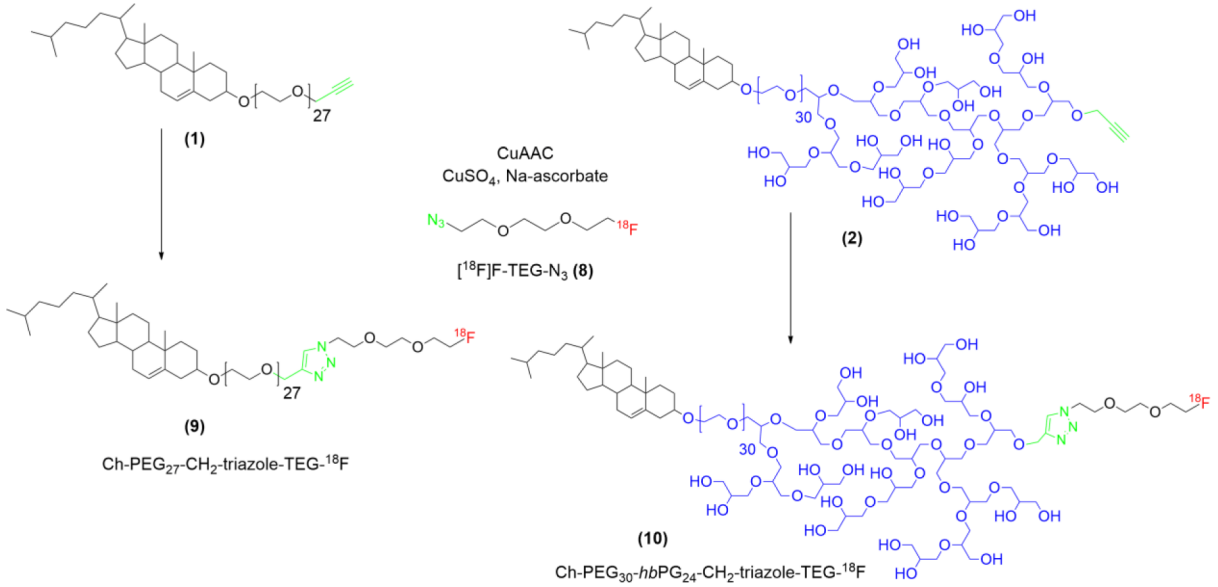

Scheme 3. Reaction Scheme for the Synthesis of 3-[^{18}F]Fluoro-cholest-5-ene (11; Abbreviated ^{18}F-Cholesten) Starting from Cholesterol

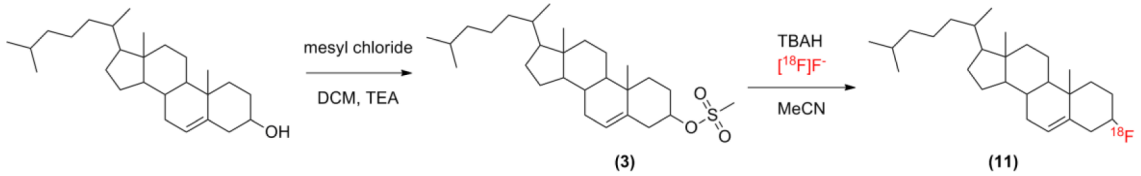

Further Syntheses. The respective reaction schemes and descriptions of labeling precursors and reference compounds (compounds **3**−**7**) are given in the Supporting Information.

Radiosyntheses. *1-Azido-2-(2-(2-[^{18}F]fluoroethoxy) ethoxy)ethane ([^{18}F]F-TEG-N$_3$; **8**).* Compound **8** (Scheme S4) was prepared on a semiautomatic custom built modular system with RCY ∼ 86% (TLC, EA/nHex (1:1), R_f: 0.8) similar to a recently presented route.[40] In a first step, the [^{18}F]fluoride was trapped on a Waters QMA light Sep-Pak cartridge (preconditioned with 10 mL of K_2CO_3 (1 M), 10 mL of Milli-Q H_2O, and 20 mL of air). To elute the activity into the reaction vessel 15 μmol K_2CO_3 and 40 μmol Kryptofix 222 in 1 mL of acetonitrile (MeCN) were used. To remove residual water, the solvent was dried azeotropically by stepwise reducing the pressure and helium flow, while the vessel was heated at 80 °C. After cooling to 40 °C and ventilation, 9.6 mg (29 μmol in 1 mL MeCN) of the tosylate precursor (**7**) were added to the reaction vessel, and the nucleophilic fluorination reaction was performed at 90 °C for 10 min. After cooling again to 40 °C, the reaction solution was quenched with 1 mL MeCN/H_2O (50:50), and the resulting 2 mL of solution was automatically transferred to the sample loop of a semipreparative HPLC (Luna 10u Prep C18(2) 100A 250 × 10.00 mm; 4 mL/min; MeCN/H_2O (50:50)). The separated fraction of (**8**; R_f: 6 min) was collected in 35 mL of Milli-Q H_2O and finally passed through a Merck Lichrolut EN cartridge (preconditioned with 10 mL MeCN, 10 mL Milli-Q H_2O and 20 mL air), followed by drying in a stream of helium. To obtain compound **8**, the cartridge was eluted with 1.5 mL of diethyl ether into a reacti-vial with septum and stirring bar. Subsequent removal of the solvent under reduced pressure and a stream of helium (850 mbar, 40 °C, He: 10 mL/min) within 8 min gave a synthon-coated vial.

*Ch-PEG$_{27}$-CH$_2$-triazole-TEG-^{18}F (**9**).* Compound **9** (Scheme 2) by CuAAC was carried out in a reacti-vial with stirring bar. A solution of 8.8 mg (5.5 μmol; **1**) in 880 μL of PBS was added directly to the synthon-coated vial. After adding 320 μL of PBS, 12.5 μL of DMSO, and 15 μL (15 μmol) of $CuSO_4$, the reaction was started by adding 22.5 μL of sodium ascorbate (49.4 mg in 100 μL PBS) and heating the reaction vial at 70 °C for 15 min under stirring. Radiochemical yields (>95%) of the triazole product were determined by TLC with EA/nHex (1:1) as mobile phase (R_f: 0, Synthon R_f: 0.8). After cooling, the reaction solution was passed through 600 mg Chelex 100 in a 3 mL SPE tube (preconditioned with 0.8 mL of HCl (1 M), 5 mL of H_2O, 0.8 mL of NaOH (1 M), 5 mL of H_2O, and 10 mL of air) followed by 7 mL of abs. EtOH to retain the copper from the reaction solvent. To confirm the absence of copper, an aliquot was taken and a few drops of sodium sulfide solution were added. The copper-free, but aqueous, ethanol containing solution was passed through a 6 mL SPE tube filled to 2/3 with anhydrous sodium sulfate (20 μm PTFE frits at top and bottom) and a 0.45 μm PTFE filter to remove the water. After flushing the self-assembled cartridge with 1 mL of abs. EtOH and 10 mL of air, the solvent was removed in a mini rotary evaporator to obtain the radiolabeled Ch-PEG$_{27}$-CH$_2$-triazole-TEG-^{18}F (**9**). Estimating the specific activity, in terms of activity per amount of polymer (μmol), gave values of 296 MBq/μmol.

*Ch-PEG$_{30}$-hbPG$_{24}$-CH$_2$-triazole-TEG-^{18}F (**10**).* Compound **10** (Scheme 2) by CuAAC was carried out in a reacti-vial with a stirring bar. A solution of 1 mg (0.28 μmol; **2**) in 100 μL of PBS was added to the vial. After adding 500 μL of PBS, 20 μL (20 μmol) of $CuSO_4$, and [^{18}F]F-TEG-N$_3$ (**8**) taken up in 400 μL of EtOH, the reaction was started by adding 40 μL of sodium ascorbate (49.4 mg in 100 μL PBS) and heating the reaction vial to 70 °C for 15 min under stirring. Radiochemical yields (>95%) of the triazole product were determined by TLC with EA/nHex (1:1) as mobile phase (R_f: 0, Synthon R_f: 0.8, see Supporting Information, Figures S6 and S7). After cooling down, the reaction solution was passed through 600 mg Chelex 100 in a 3 mL SPE tube (preconditioned with 0.8 mL of HCl (1 M), 5 mL of H_2O, 0.8 mL of NaOH (1 M), 5 mL of H_2O, and 10 mL of air), followed by 7 mL of abs. EtOH to remove the copper from the

DOI: 10.1021/bm5017332
Biomacromolecules 2015, 16, 842−851

reaction solvent. To confirm the absence of copper, an aliquot was taken and a few drops of sodium sulfide solution were added. The copper-free solution was passed through a 6 mL SPE tube filled to 2/3 with anhydrous sodium sulfate (20 μm PTFE frits at top and bottom) and a 0.45 μm PTFE filter to remove the water. After flushing the self-assembled cartridge with 1 mL of abs. EtOH and 10 mL of air, the solvent was removed in a mini rotary evaporator to obtain the radiolabeled Ch-PEG_{30}-*hb*PG_{24}-CH_2-triazole-TEG-^{18}F (**10**). Estimating the specific activity, in terms of activity per used polymer (μmol), gave values of 8.72 GBq/μmol.

3-[^{18}F]Fluoro-cholest-5-ene (11). Compound **11** (Scheme 3) was prepared by direct fluorination of the mesylated cholesterol precursor (**3**) with RCY ∼ 25%. [^{18}F]Fluoride was trapped on a Waters QMA light Sep-Pak cartridge (preconditioned with 10 mL of K_2CO_3 (1 M), 10 mL of Milli-Q H_2O, and 20 mL of air). After eluting the activity with 0.9 mL (52 μmol) of TBAH in MeOH into a septum-sealed reacti-vial, the solution was dried under reduced pressure and a stream of helium (260 mbar, 85 °C, 200 mL/min He). Residual water was removed azeotropically by adding 1 mL of MeCN (3×) under above-mentioned conditions. Compound **3** (9.3 mg, 20 μmol) dissolved in 1 mL of MeCN was added directly to the vial and heated for 20 min at 120 °C. During cool down in cold water for 5 min, the solution was quenched with 2-propanol (1 mL), followed by purification via semipreparative HPLC (Luna 10u Prep C18(2) 100A 250 × 10.00 mm; 4 mL/min; *i*PrOH/MeCN (80:20)). The solvents of the separated fraction were removed within 10 min using a mini rotary evaporator (stepwise reducing pressure, starting with 200 mbar, 45 °C). Radiochemical yields of **11** were determined by RP-TLC (Merck TLC Silica gel 60 RP-18 F254s) with *i*PrOH/MeCN (4:1) as mobile phase (R_f: 0.4, see Supporting Information, Figure S8). Compound **11** was identified in HPLC and TLC via the reference compound **4**. The specific activity of **11** was determined to be >4.2 GBq/μmol by analytical HPLC (Luna 5u C18(2) 250 × 4.6 mm, 0.5 mL/min; *i*PrOH/MeCN/H_2O (80:18:2). The nonradioactive ^{19}F-Cholesten was used to determine the lowest amount of substance that can be detected by UV (210 nm). For taking up **11** into an injectable phosphate buffered saline solution, (2-hydroxypropyl)-β-cyclodextrin (45% (w/v) solution in water) was used as a solubilizer. For the liposome preparation, no solubilizer was used.

RESULTS AND DISCUSSION

Polymer Syntheses and Radioactive Labeling with [^{18}F]Fluorine via CuAAC-Reaction. As described above, this work aims at the investigation of the in vivo behavior and biodistribution of two fundamentally different polymers and their liposomal formulations that are sterically stabilized: (i) linear poly(ethylene glycol) (PEG) with a cholesterol anchor and (ii) linear-hyperbranched polyglycerol (PEG-*hb*PG) with a cholesterol anchor group. Both polymers differ in the number of hydroxyl groups and the polymer architecture (linear vs linear-hyperbranched, Scheme 2). A special focus was placed on the radiolabeling of the polymers in order to follow the polymers' fate in vivo. The polyether-based amphiphiles were synthesized according to the literature, using cholesterol as a hydrophobic initiator for the oxyanionic ring-opening polymerization of a combination of epoxides.[14−16] Molecular weights were chosen to be between 1500 and 3500 g mol^{-1}, which is common for sterically stabilized liposomes.[41] The renal threshold for PEG is known to be around 40000 g mol^{-1} (M_w); thus, fast excretion of the lipids from the body was assumed.[42]

In order to attach the positron emitter fluorine-18 ($t_{1/2}$ = 109.7 min) to the polyether backbone, the polymers were functionalized with propargyl bromide. 1-Azido-2-(2-(2-[^{18}F]-fluoroethoxy)ethoxy)ethane ([^{18}F]F-TEG-N_3, **8**) was used as the synthon for click-chemistry, which made both ex vivo organ distribution measurements as well as μPET imaging of the polymers possible. For the hyperbranched polymer Ch-PEG_{30}-*hb*PG_{24}-CH_2-C≡CH, the general synthesis and functionalization was recently published by our group.[15,43] The number of alkyne groups can be tailored by the amount of propargyl bromide utilized, albeit a statistical distribution at the polymer chains is inevitable. From ^{1}H NMR spectroscopy, 1−2 alkyne groups per polymer chain were calculated. The linear analogue was prepared by the oxyanionic ring-opening polymerization of ethylene oxide (EO) using cholesterol as an initiator. Direct end-capping of the oxyanion with propargyl bromide led to the functionalized Ch-PEG_{27}-CH_2-C≡CH (**1**) polymer (Scheme 1).

Both polymers were characterized by ^{1}H NMR spectroscopy and size exclusion chromatography (SEC). Ch-PEG_{27}-CH_2-C≡CH (**1**) revealed a molecular weight of $M_{n,NMR}$ = 1600 g mol^{-1} and a narrow molecular weight distribution of M_w/M_n = 1.13 ($M_{n,SEC}$ = 1500 g mol^{-1}). The molecular weight of Ch-PEG_{30}-*hb*PG_{24}-CH_2-C≡CH (**2**) was $M_{n,NMR}$ = 3520 g mol^{-1} (calculated by ^{1}H NMR spectroscopy), and SEC revealed a distribution of M_w/M_n = 1.14 ($M_{n,SEC}$ = 1550 g mol^{-1}). The molecular weight determined by SEC is underestimated due to the globular polymer structure and consequently lower hydrodynamic radius compared to the SEC standard PEG. The ^{1}H NMR spectrum for the linear and linear-hyperbranched polyether is given in Figures S1 and S2 (Supporting Information). Furthermore, MALDI-ToF mass spectrometry was employed to confirm the introduction of cholesterol and the alkyne group at every polymer chain, which is crucial for the functionalization with the radioactive compound in the subsequent click reaction (Supporting Information, Figure S3).

The synthon [^{18}F]F-TEG-N_3 (**8**) was prepared via a slightly modified route, based on the approach recently presented by Rokka et al.[40] The synthesis was carried out in a semi-automated, custom-built modular system. Starting from a tosylate precursor, the nucleophilic fluorination reaction was carried out with a good radiochemical yield (RCY) of 86%. The preparation is explained in the Experimental Section, and the reaction scheme is given in Schemes S3 and S4 (Supporting Information). The main advantages of using fluorine-18 are its outstanding physical and nuclear properties, resulting in high spatial resolution compared to other PET nuclides and temporal resolution. Due to its size and lack of charge, no influence on the polymer conformation and hydrodynamic properties is assumed. Furthermore, the rather small molecule [^{18}F]F-TEG-N_3, having an oligoether structure, is believed to be ideal for the attachment onto polyether-based lipids.

The copper-catalyzed azide−alkyne cycloaddition reaction (CuAAC) between the alkyne-functionalized polymers and the radioactive azide compound was carried out in (ethanolic) aqueous solution with a radiochemical yield (RCY) of >95% for the linear and the linear-hyperbranched lipid. The chemical structures and the overall strategy are presented in Scheme 2. Cu(I) was prepared in situ through the reduction of copper(II) sulfate by sodium ascorbate. During optimization of the reactions, a strong variation of yields was observed, based on the ratio of catalyst to ascorbate and on the amount of copper itself. In addition, the solvent played an important role. Phosphate buffered saline was superior to water, whereas DMSO also gave very good yields. Because of the difficulties to remove DMSO (high boiling point) subsequent to the reaction in order to form a lipid film for the liposome preparation, the solvent system of choice was PBS and EtOH (a small selection of the differing reaction parameters is given in Table S1).

DOI: 10.1021/bm5017332
Biomacromolecules 2015, 16, 842−851

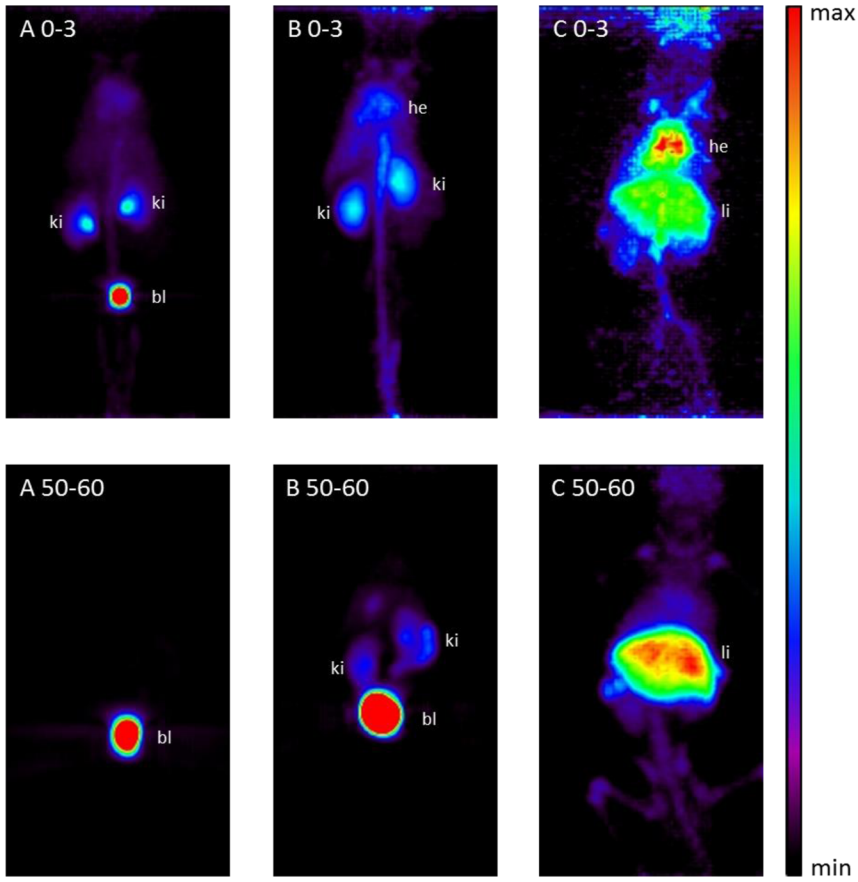

Figure 2. MIPs (coronal view) of whole body distribution for early (0−3 min) and late (50−60 min) time frames of Ch-PEG_{27}-CH_2-triazole-TEG-^{18}F (A), Ch-PEG_{30}-*hb*PG_{24}-CH_2-triazole-TEG-^{18}F (B), and ^{18}F-cholestene (C); ki: kidney, bl: bladder, he: heart, li: liver.

Main advantages of the rapid attachment of fluorine-18 to the stabilizing polymers compared to the already mentioned strategies are (i) fast click-reaction with high yields, (ii) the novel shielding polymer itself is labeled instead of lipids such as [^{18}F]FDP, (iii) incorporation of the polyether-based lipid into liposomes can be directly monitored, and (iv) the behavior and fate of the polymer itself can be investigated in vivo to study the excretion rate and pathway.

Radioactive Labeling of Cholesterol. In addition to the radiolabeling of the polyether lipids, labeling of cholesterol with fluorine-18 was successfully carried out. Nozaki et al. and Fukushi et al. mentioned a labeled cholesterol compound in the 60s and 70s, synthesized via AgF, but a detailed description is missing.[44,45] In the present case, the synthesis by direct labeling of the mesylated form of cholesterol was achieved. Starting from commercially available cholesterol (see Scheme 3), methanesulfonyl chloride was reacted with the hydroxyl group of cholesterol in order to introduce the leaving group in the first step. In the second step, a nucleophilic substitution was carried out using ^{18}F-fluoride and the tetrabutylammonium hydroxide (TBAH) system. 3-[^{18}F]Fluoro-cholest-5-ene (**11**) was obtained with RCYs around 25%. While performing radiolabeling, characterization, and purification, challenges with respect to solubility were observed. The labeling reaction can be carried out in DMSO as well, but the purification via semipreparative HPLC (*i*PrOH/MeCN as liquid phase) was not possible due to a lack of retention of the fluoro-cholestene caused by the solvent. Diluting the reaction with sufficient amounts of water was also not possible. To avoid these points, labeling was performed in MeCN.

Critical Micelle Concentration and Liposome Formation. In order to investigate potential polymer micelle formation in the bloodstream, the linear polyether as well as the linear-hyperbranched polyether were characterized by surface tension measurements. Based on the amphiphilic character of the polymers, their critical micelle concentrations (CMC) were determined to be 7.9 mg L^{-1} for the linear and 11.0 mg L^{-1} for the branched structure using a ring tensiometer. This is in line with expectation, since the latter polymer is more hydrophilic due to multiple hydroxyl groups and therefore should exhibit an increased CMC compared to linear PEG. For mice having a blood volume of about 1.6−2.4 mL (20−30 g body weight),[46] this means that, for a solution of free polymer in buffer with 1 mg mL^{-1}, micelle formation can be expected in vivo. The size of the micelles was studied with dynamic light scattering (DLS), and a hydrodynamic radius (R_h) of 6.9 nm for both polymers was found.

Liposomes consisting of Ch-PEG_{27}-CH_2-triazole-TEG-^{18}F, Ch-PEG_{30}-*hb*PG_{24}-CH_2-triazole-TEG-^{18}F, or ^{18}F-cholestene, DOPC, and cholesterol were prepared by the thin film hydration method and extrusion through polycarbonate membranes (400 and 100 nm). To purify the liposomes from nonintegrated lipids SEC was carried out. DLS was performed to evaluate the size of the liposomes after the radioactivity was decayed. The error for these DLS measurements is between 2 and 10%. For liposomes that are stabilized by the linear polymer (20 mol %), R_h was determined to be 46 nm. For the

DOI: 10.1021/bm5017332
Biomacromolecules 2015, 16, 842−851

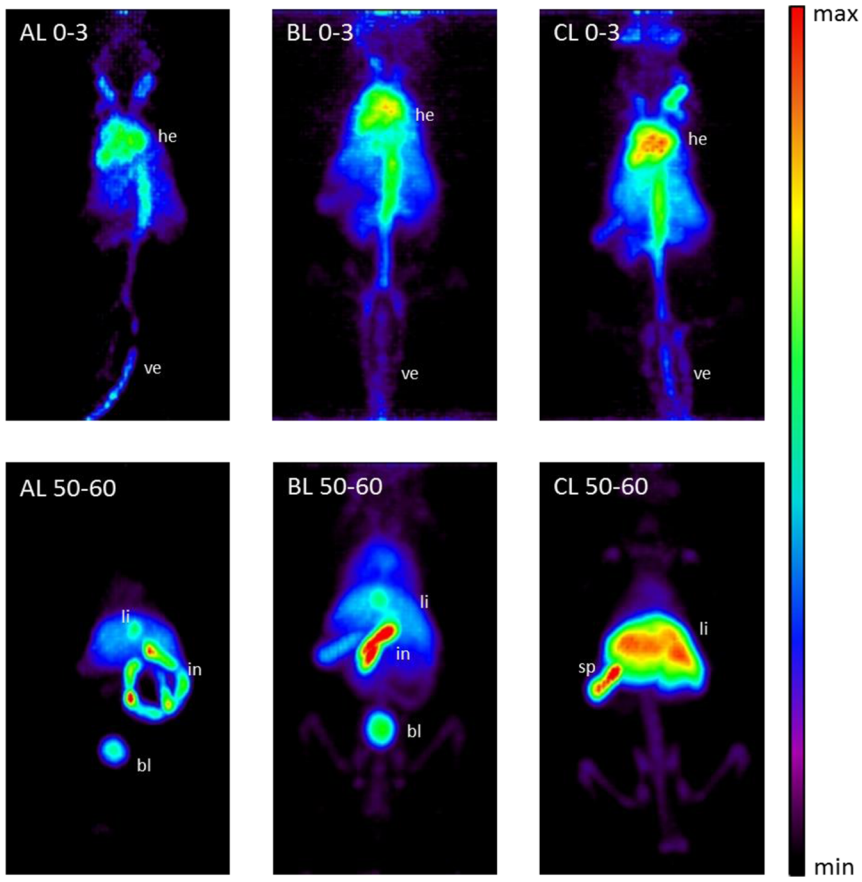

Figure 3. MIPs (coronal view) of whole body distribution for early (0−3 min) and late (50−60 min) time frames of Ch-PEG_{27}-CH_2-triazole-TEG-^{18}F Lipo 20 mol % (AL), Ch-PEG_{30}-*hb*PG_{24}-CH_2-triazole-TEG-^{18}F Lipo 20 mol % (BL), and ^{18}F-cholestene Lipo (CL); he: heart, ve: vein, li: liver, in: intestine, sp: spleen, bl: bladder.

linear-hyperbranched polymers stabilizing the liposomes, higher radii were found, that is, $\langle 1/R_h \rangle_z^{-1}$ = 86 nm (5 mol %) and $\langle 1/R_h \rangle_z^{-1}$ = 83 nm (20 mol % polymer). These values are almost twice as high as for the PEGylated liposomes, although all suspensions were extruded through a 100 nm membrane in the same manner. These differences in size are due to the different sterical demand of the shielding polymers in combination with the extrusion technique. Conventional liposomes containing ^{18}F-cholestene exhibited even larger sizes ($\langle 1/R_h \rangle_z^{-1}$ = 204 nm) due to the lack of a surface-stabilizing polymer. These results emphasize the importance of a stabilizing and shielding polymer anchored to the liposomes as drug delivery vehicles.

Animal Studies. *PET Imaging.* To investigate the dynamics of the initial biodistribution of the different compounds in vivo, μPET experiments were performed over 60 min in mice. Figure 2 A, B, and C show coronal views of maximum intensity projections (MIPs) of early (0−3 min) and late (50−60 min) time frames of the linear polymer (Ch-PEG_{27}-CH_2-triazole-TEG-^{18}F), the linear-hyperbranched polyether (Ch-PEG_{30}-*hb*PG_{24}-CH_2-triazole-TEG-^{18}F), and of ^{18}F-cholestene, respectively. While the linear (A) and linear-hyperbranched (B) polymers, which are assumed to form micelles, are eliminated quickly via the renal excretion pathway, ^{18}F-cholestene (C) shows mainly uptake in the liver, as expected due to its hydrophobic character and the bile acid synthesis. Defluorination can be seen to a minor extent in the late time frames by [^{18}F]F^- uptake of the bones. The renal clearance of the linear-hyperbranched structure from the blood clearly exhibits slower kinetics than for the linear structure. Nevertheless, it is important to note that almost complete body clearance of the polymers is observed after 1 h, and no accumulation in the MPS system is observed. The polymers' fate is only detectable since the polymer micelles are labeled, which enables tracing of these structures.

In comparison to these observations, Figure 3 depicts the liposomal formulations of the above-mentioned compounds during the same time frames, abbreviated as AL, BL, and CL. Molar ratios of the liposomes containing Ch-PEG_{27}-CH_2-triazole-TEG-^{18}F and Ch-PEG_{30}-*hb*PG_{24}-CH_2-triazole-TEG-^{18}F (AL and BL) were DOPC/cholesterol/polymer (60:20:20). For ^{18}F-cholestene (CL) it was DOPC/cholesterol (60:40) plus the labeled cholesterol to keep the molar percentage of cholesterol and lipid constant. It is obvious that the liposome biodistribution exhibits a clearly different pattern compared to the polymer micelles. The extent of renal clearance of the linear (AL) and linear-hyperbranched (BL) sterically stabilized liposomes is considerably lower than for the polymer micelles. Instead, only low uptake in the liver and intestines is observed. However, the biodistribution of the liposomal ^{18}F-cholestene (CL) does not differ much from the single molecule. In the late time frame (CL 50−60) an increased uptake in the spleen can be observed, compared to the late time frame in Figure 2 (C 50−60).

Ex Vivo Biodistribution. To obtain a quantitative statement concerning the trafficking of the radiolabeled compounds an ex vivo biodistribution study was performed.

DOI: 10.1021/bm5017332
Biomacromolecules 2015, 16, 842−851

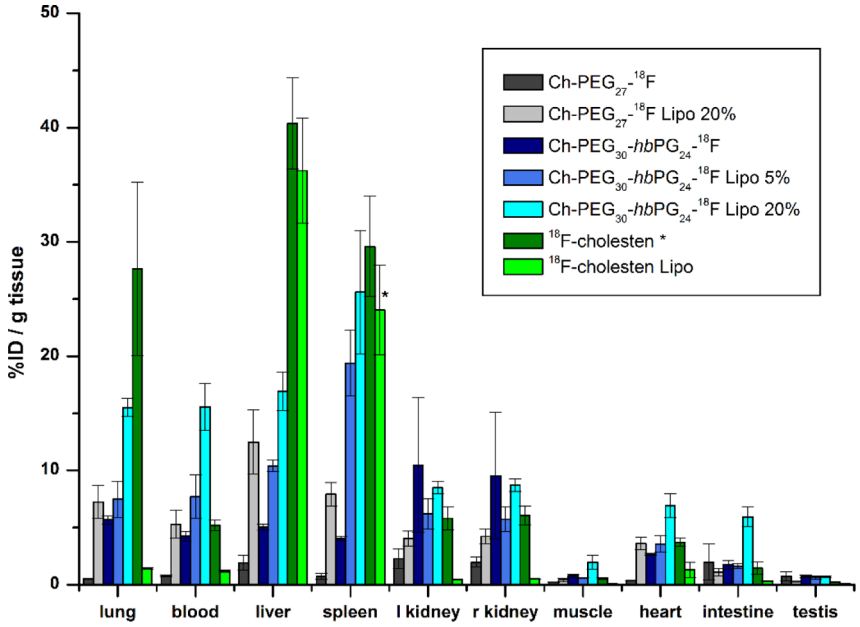

Figure 4. Graphical summary of ex vivo biodistribution data (n = 3) of male C57bl6J mice 1 h p.i. Asterisk indicates n = 2. Liposomal formulations are abbreviated with Lipo. x % is the molar percentage of the polymer added to the DOPC−cholesterol mixture (60:40-x:x), with x = 5 or 20, theoretical values. Error values are given as standard error of the mean. Data of urine is not shown to obtain a clear survey, but the values are given in Table S2. For saving space, the abbreviation "CH_2-triazole-TEG" is left out in the legend.

Figure 4 summarizes these results for the radiolabeled compounds Ch-PEG_{27}-CH_2-triazole-TEG-^{18}F (**9**), Ch-PEG_{30}-*hb*PG_{24}-CH_2-triazole-TEG-^{18}F (**10**), and ^{18}F-cholestene (**11**), as well as the liposomal formulation of the above-mentioned cholesterol derivatives in male C57bl6J mice (24.8 ± 1.9 g) 1 h post-injection.

Table S2 gives an overview of all data, whereas the data of urine is not shown in Figure 4 for clarity. Similar to the PET images, the linear and linear−hyperbranched polymer itself (micelles) showed fast renal clearance, which was confirmed by high amounts of radioactivity in the urine (>300%ID/g). Fast renal clearance of the polymers and no accumulation in organs is desired, as this represents the preferential elimination pathway subsequent to degradation of the liposomes. The linear-hyperbranched structure showed slightly increased retention in blood, lung, liver, spleen, and kidneys, which can be attributed to differences in micelle surface properties of the branched polymer compared to linear PEG. Nevertheless, values for the kidneys were around 10%ID/g, which indicates fast renal clearance. ^{18}F-Cholestene is mainly retained in liver, spleen, and lung (%ID/g > 27, Figure 4) and, as expected, shows almost no renal excretion due to its hydrophobic character.

The biodistribution patterns of the sterically stabilized liposomes with Ch-PEG_{30}-*hb*PG_{24}-CH_2-triazole-TEG-^{18}F (5 and 20 mol %) or Ch-PEG_{27}-CH_2-triazole-TEG-^{18}F Lipo (20 mol %) differ from the polymer micelles, as summarized in Figure S9. For liposomes stabilized with PEG-lipids values of 28.46 ± 1.49%ID/g were found in the urine, which is much less than for PEG-lipid micelles with 1070 ± 141%ID/g. The different pattern hints indirectly at successful incorporation of the polymer into the liposomes and therefore advantageous biodistribution, which translates to longer retention times in the body. PEG-liposomes showed increased values in lung, liver, and spleen, but most importantly also in blood (5.30 ± 1.24%ID/g) and heart (3.60 ± 0.52%ID/g). For liposomes stabilized with the linear-hyperbranched lipids, values of 221 ± 48%ID/g (5 mol % polymer) and 26.46 ± 12.40%ID/g (20 mol % polymer) were found in the urine (Table S2). The first result points to insufficient incorporation of the bulky lipid into the liposomes for this concentration. Therefore, the amount of polymer employed prior to extrusion was raised to 20 mol % (theoretical value, see also discussion below), maintaining the liposome size. Renal clearance was suppressed dramatically, showing comparable values to the PEGylated liposomes (26.46 vs 28.46%ID/g) and retention in liver, lung, and spleen was observed. Simultaneously, retention in the bloodstream (15.56 ± 2.50%ID/g) and heart (6.91 ± 1.05%ID/g) after 1 h was enhanced. Compared to the linear structures, the linear-hyperbranched shielded liposomes show higher retention in well perfused tissue, like the lung and blood, but comparable values in the liver. Uptake in the spleen is increased for linear-hyperbranched liposomes versus the linear ones, indicating increased uptake into the MPS.

As expected, nonstabilized liposomes accumulate strongly in the liver and the spleen (>24%ID/g, Table S2, Figure 4), which is attributed to fast removal from the bloodstream by macrophages (MPS uptake) due to liposome size and possible aggregation with proteins. A comparison of the three types of liposomes is shown in Figure S10.

Approximate Determination of Polymer Incorporation. The reason for increasing the amount of polymer lipid added to the lipid−cholesterol mixture before sonification and extrusion was the rather rapid elimination in case of the 5 mol % linear-hyperbranched liposome formulation. To estimate the degree of integration of the shielding polymer lipid, the elution profile of the SEC after extrusion was recorded. The activity of each fraction was measured and decay-corrected. Furthermore, the remaining activity of the SEC column was determined. By dividing the accumulated liposomal fractions by the total activity, the degree of integration was estimated. Because the linear-hyperbranched polymer was incorporated into the lipid

DOI: 10.1021/bm5017332
Biomacromolecules 2015, 16, 842−851

bilayer only between 20 and 30% according to our calculations, we scaled up the amount of polymer from 5 to 20 mol %. The linear polymer and ^{18}F-cholestene were incorporated in higher quantities that are ~60% and ~85%, respectively, probably due to their less sterically demanding architecture. Of course, these findings are only rough values, but once more emphasize the advantage of labeling the shielding polymer for control of integration instead of incorporating a radioactive probe into the liposome membrane.

Comparison between Linear and Linear-Hyperbranched Stabilized Liposomes. Comparing the 20 mol % liposomes of the linear with the linear-hyperbranched polymer lipids, the hyperbranched polyglycerol units lead to higher uptake in lung, blood, liver, and spleen. Figure 5 depicts the ratios of blood-to-organ for these two formulations.

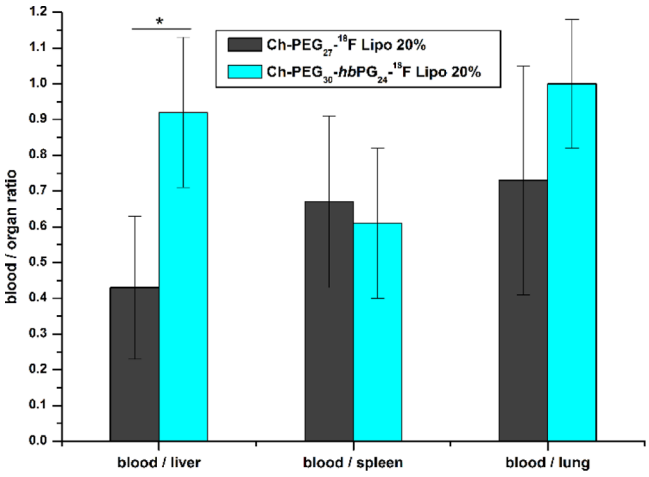

Figure 5. Blood-to-organ ratios (ex vivo biodistribution data) of liposomal formulations (20 mol %, theoretical) of Ch-PEG$_{27}$-CH$_2$-triazole-TEG-^{18}F (gray) and Ch-PEG$_{30}$-*hb*PG$_{24}$-CH$_2$-triazole-TEG-^{18}F (cyan). In order to save space, the abbreviation "CH$_2$-triazole-TEG" is left out in the legend. Error values are calculated by error propagation of standard errors of the mean. Asterisk indicates $P < 0.05$.

It is obvious from Figure 5 that liposomes with linear-hyperbranched shielding are superior considering blood-to-liver ratios. Furthermore, they show comparable ratios in blood-to-spleen and slightly better blood-to-lung ratios in comparison to the linear shielded liposomes.

Besides the type of shielding, the size of the liposomes has to be taken into consideration. It is believed that liposomes smaller than 100 nm are opsonized less quickly and to a lower extent compared to liposomes with sizes exceeding 100 nm. Hence, the liposome uptake by the MPS increases with the size of the vesicles.[1] Unfortunately, even though they were all extruded through the same pore size, the size of the investigated liposomes differed. Showing a hydrodynamic radius of 46 nm, the linear shielded liposomes were the smallest structures, followed by the linear-hyperbranched shielded liposomes with $\langle 1/R_h \rangle_z^{-1}$ = 83 and 204 nm for the conventional liposomes. Comparing these sizes, the linear-hyperbranched shielded liposomes may show even more advantageous behavior in vivo if the liposome sizes can be reduced below 100 nm in diameter.

The findings confirm that both polyether architectures are advantageous for drug delivery applications, with the hyper-branched structure introducing additional multifunctionality at the liposome surface.

CONCLUSION

This study presents a novel method for labeling polyether-based lipids and in vivo tracking conventional and sterically stabilized liposomes by ^{18}F-labeling of cholesterol or the respective polymers. The labeled systems were injected into C57bl6J mice and tracked by noninvasive μPET for 1 h. The positron emitting isotope fluorine-18 enabled PET imaging with high spatial resolution compared to other PET nuclides. With its lack of charge and similarity in structure to the polyether backbone of the polymer, the clickable label is believed not to affect the polymeric structure as much as a chelator. Radiolabeling of the polymers via copper-catalyzed click reaction, instead of labeling the phospholipids, allowed not only for the investigation of the fate of the liposomes, but also permitted to monitor the polymer micelles' fate in vivo and, thus, enabled an assessment of the impact of the liposome superstructure. The time frame used in this study is, of course, too short to prove an enhanced permeability and retention (EPR) effect. Nevertheless, this technique is versatile and suitable to investigate initial body distribution of polymer amphiphiles and polymer-stabilized liposomes. In addition to these observations, a generally usable probe, ^{18}F-cholestene, for liposome labeling was introduced. The architecture and therefore the number of functionalities, the amount of polymer, and the liposome size play an important role for the biodistribution pattern. As expected, conventional liposomes showed major MPS uptake, which confirms the need for a stabilizing polymer for these drug delivery systems. The "gold standard" PEG with a cholesterol anchor group exhibited satisfying results with moderate retention in lung, blood, liver, and spleen. Blood retention was the highest for linear-hyperbranched lipids incorporated into liposomes with 20 mol % (theoretical value) via a cholesterol anchor. These results demonstrate the advantageous properties of the novel polyether-based lipids, which combine multifunctionality and steric stabilization of vesicles. By using a very small radionuclide and respective PET measurements, fast noninvasive screening and comparison of the body distribution of different polymer architectures and their supramolecular structures was possible.

ASSOCIATED CONTENT

Supporting Information

Reaction schemes and analytics of organic and radiochemical syntheses and ex vivo biodistribution data. This material is available free of charge via the Internet at http://pubs.acs.org.

AUTHOR INFORMATION

Corresponding Authors

*E-mail: hfrey@uni-mainz.de. Phone: +49 6131 39 24078. Fax: +49 6131 39 26106.

*E-mail: froesch@uni-mainz.de. Phone: +49 6131 39 25302. Fax: +49 6131 39 25253.

Author Contributions

‡These authors contributed equally (A.T.R. and S.S.M.).

Notes

The authors declare no competing financial interest.

DOI: 10.1021/bm5017332
Biomacromolecules 2015, 16, 842−851

■ ACKNOWLEDGMENTS

The authors would like to thank Dr. Hanno Schieferstein for assistance during radiosyntheses. Our gratitude also belongs to Sabine Gietzen for DLS measurements. S.S.M. is a recipient of a fellowship through the Excellence Initiative (DFG/GSC 266) and part of the graduate school MAINZ. We also acknowledge financial support from the DFG in the context of the SFB 1066 ("Nanodimensional Polymer Therapeutics for Tumor Therapy"). A.T.R. is part of the graduate school of SFB 1066.

■ REFERENCES

(1) Sharma, A.; Sharma, U. S. *Int. J. Pharm.* **1997**, *154*, 123−140.
(2) Torchilin, V. P. *Nat. Rev. Drug Discovery* **2005**, *4*, 145−160.
(3) Harashima, H.; Sakata, K.; Funato, K.; Kiwada, H. *Pharm. Res.* **1994**, *11*, 402−406.
(4) Lasic, D. D.; Needham, D. *Chem. Rev.* **1995**, *95*, 2601−2628.
(5) Immordino, M. L.; Dosio, F.; Cattel, L. *Int. J. Nanomed.* **2006**, *1*, 297−315.
(6) Torchilin, V. P.; Omelyanenko, V. G.; Papisov, M. I.; Bogdanov, A. A.; Trubetskoy, V. S.; Herron, J. N.; Gentry, C. A. *Biochim. Biophys. Acta, Biomembr.* **1994**, *1195*, 11−20.
(7) Knop, K.; Hoogenboom, R.; Fischer, D.; Schubert, U. S. *Angew. Chem., Int. Ed.* **2010**, *49*, 6288−6308.
(8) Torchilin, V. P.; Shtilman, M. I.; Trubetskoy, V. S.; Whiteman, K.; Milstein, A. M. *Biochim. Biophys. Acta, Biomembr.* **1994**, *1195*, 181−184.
(9) Zalipsky, S.; Hansen, C. B.; Oaks, J. M.; Allen, T. M. *J. Pharm. Sci.* **1996**, *85*, 133−137.
(10) García, K. P.; Zarschler, K.; Barbaro, L.; Barreto, J. a.; O'Malley, W.; Spiccia, L.; Stephan, H.; Graham, B. *Small* **2014**, *10*, 2516−2529.
(11) Siegers, C.; Biesalski, M.; Haag, R. *Chem.—Eur. J.* **2004**, *10*, 2831−2838.
(12) Yeh, P.-Y. J.; Kainthan, R. K.; Zou, Y.; Chiao, M.; Kizhakkedathu, J. N. *Langmuir* **2008**, *24*, 4907−4916.
(13) Maruyama, K.; Okuizumi, S.; Ishida, O.; Yamauchi, H.; Kikuchi, H.; Iwatsuru, M. *Int. J. Pharm.* **1994**, *111*, 103−107.
(14) Hofmann, A. M.; Wurm, F.; Hühn, E.; Nawroth, T.; Langguth, P.; Frey, H. *Biomacromolecules* **2010**, *11*, 568−574.
(15) Hofmann, A. M.; Wurm, F.; Frey, H. *Macromolecules* **2011**, *44*, 4648−4657.
(16) Müller, S. S.; Dingels, C.; Hofmann, A. M.; Frey, H. *ACS Symp. Ser.* **2013**, *1135*, 11−25.
(17) He, Z.-Y.; Chu, B.-Y.; Wei, X.-W.; Li, J.; Edwards, C. K.; Song, X.-R.; He, G.; Xie, Y.-M.; Wei, Y.-Q.; Qian, Z.-Y. *Int. J. Pharm.* **2014**, *469*, 168−178.
(18) Mohr, K.; Müller, S. S.; Müller, L. K.; Rusitzka, K.; Gietzen, S.; Frey, H.; Schmidt, M. *Langmuir* **2014**, *30*, 14954−14962.
(19) Phillips, W. T.; Rudolph, A. S.; Goins, B.; Timmons, J. H.; Klipper, R.; Blumhardt, R. *Nucl. Med. Biol.* **1992**, *19*, 539−547.
(20) Bao, A.; Goins, B.; Klipper, R.; Negrete, G.; Phillips, W. T. *J. Nucl. Med.* **2003**, *44*, 1992−1999.
(21) Mauk, M. R.; Gamble, R. C. *Anal. Biochem.* **1979**, *94*, 302−307.
(22) Harrington, K. J.; Mohammadtaghi, S.; Uster, P. S.; Glass, D.; Peters, A. M.; Vile, R. G.; Stewart, J. S. *Clin. Cancer Res.* **2001**, *7*, 243−254.
(23) Gaspar, M. M.; Boerman, O. C.; Laverman, P.; Corvo, M. L.; Storm, G.; Cruz, M. E. M. *J. Controlled Release* **2007**, *117*, 186−195.
(24) Seo, J. W.; Zhang, H.; Kukis, D. L.; Meares, C. F.; Ferrara, K. W. *Bioconjugate Chem.* **2008**, *19*, 2577−2584.
(25) Oku, N.; Yamashita, M.; Katayama, Y.; Urakami, T.; Hatanaka, K.; Shimizu, K.; Asai, T.; Tsukada, H.; Akai, S.; Kanazawa, H. *Int. J. Pharm.* **2011**, *403*, 170−177.
(26) Phillips, W. T.; Goins, B. A.; Bao, A. *Wiley Interdiscip. Rev. Nanomed. Nanobiotechnol.* **2009**, *1*, 69−83.
(27) Petersen, A. L.; Hansen, A. E.; Gabizon, A.; Andresen, T. L. *Adv. Drug Delivery Rev.* **2012**, *64*, 1417−1435.
(28) Seo, J. W.; Mahakian, L. M.; Kheirolomoom, A.; Zhang, H.; Meares, C. F.; Ferdani, R.; Anderson, C. J.; Ferrara, K. W. *Bioconjugate Chem.* **2010**, *21*, 1206−1215.
(29) Jacobson, O.; Kiesewetter, D. O.; Chen, X. *Bioconjugate Chem.* **2015**, *26*, 1−18.
(30) Hühn, E.; Buchholz, H.-G.; Shazly, G.; Maus, S.; Thews, O.; Bausbacher, N.; Rösch, F.; Schreckenberger, M.; Langguth, P. *Eur. J. Pharm. Sci.* **2010**, *41*, 71−77.
(31) Efferth, T.; Langguth, P. *Radiat. Oncol.* **2011**, *6*, 59.
(32) Oku, N.; Tokudome, Y.; Tsukada, H.; Kosugi, T.; Namba, Y.; Okada, S. *Biopharm. Drug Dispos.* **1996**, *17*, 435−441.
(33) Oku, N. *Adv. Drug Delivery Rev.* **1999**, *37*, 53−61.
(34) Marik, J.; Tartis, M. S.; Zhang, H.; Fung, J. Y.; Kheirolomoom, A.; Sutcliffe, J. L.; Ferrara, K. W. *Nucl. Med. Biol.* **2007**, *34*, 165−171.
(35) Urakami, T.; Akai, S.; Katayama, Y.; Harada, N.; Tsukada, H.; Oku, N. *J. Med. Chem.* **2007**, *50*, 6454−6457.
(36) Emmetiere, F.; Irwin, C.; Viola-Villegas, N. T.; Longo, V.; Cheal, S. M.; Zanzonico, P.; Pillarsetty, N.; Weber, W. A.; Lewis, J. S.; Reiner, T. *Bioconjugate Chem.* **2013**, *24*, 1784−1789.
(37) Jensen, A. T. I.; Binderup, T.; Andresen, T. L.; Kjær, A.; Rasmussen, P. H. *J. Liposome Res.* **2012**, *22*, 295−305.
(38) Workman, P.; Aboagye, E. O.; Balkwill, F.; Balmain, A.; Bruder, G.; Chaplin, D. J.; Double, J. A.; Everitt, J.; Farningham, D. A. H.; Glennie, M. J.; Kelland, L. R.; Robinson, V.; Stratford, I. J.; Tozer, G. M.; Watson, S.; Wedge, S. R.; Eccles, S. A. *Br. J. Cancer* **2010**, *102*, 1555−1577.
(39) Fitton, A. O.; Hill, J.; Jane, D. E.; Millar, R. *Synthesis* **1987**, *12*, 1140−1142.
(40) Rokka, J.; Snellman, A.; Zona, C.; La Ferla, B.; Nicotra, F.; Salmona, M.; Forloni, G.; Haaparanta-Solin, M.; Rinne, J. O.; Solin, O. *Bioorg. Med. Chem.* **2014**, *22*, 2753−2762.
(41) Woodle, M. C.; Lasic, D. D. *Biochim. Biophys. Acta, Rev. Biomembr.* **1992**, *1113*, 171−199.
(42) Pasut, G.; Veronese, F. M. *Prog. Polym. Sci.* **2007**, *32*, 933−961.
(43) Fritz, T.; Hirsch, M.; Richter, F. C.; Müller, S. S.; Hofmann, A. M.; Rusitzka, K. A. K.; Markl, J.; Massing, U.; Frey, H.; Helm, M. *Biomacromolecules* **2014**, *15*, 2440−2448.
(44) Nozaki, T.; Shimamura, A.; T, K. *IPCR Cyclotron Prog. Rep.* **1968**, 156−158.
(45) Fukushi, K.; Irie, T.; Nozaki, T.; Ido, T.; Kasida, Y. *J. Labelled Compd. Radiopharm.* **1979**, *16*, 49−51.
(46) Barbee, R. W.; Perry, B. D.; Ré, R. N.; Murgo, J. P. *Am. J. Physiol.* **1992**, *263*, R728−R733.

DOI: 10.1021/bm5017332
Biomacromolecules 2015, 16, 842−851